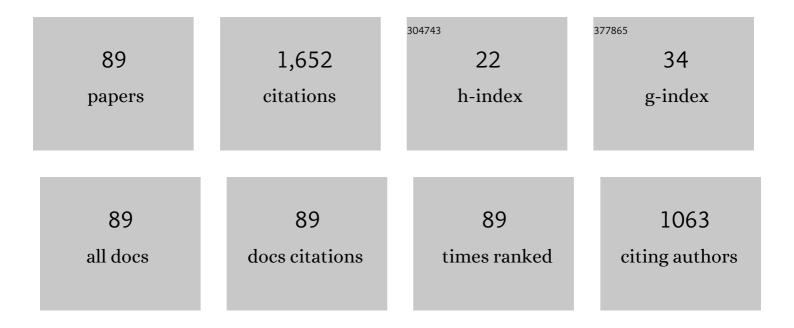
List of Publications by Year in descending order

Source: https://exaly.com/author-pdf/3590229/publications.pdf Version: 2024-02-01



#	Article	IF	CITATIONS
1	Ultrasensitive, Highly Stable, and Flexible Strain Sensor Inspired by Nature. ACS Applied Materials & Interfaces, 2022, 14, 16885-16893.	8.0	23
2	Preparation and property optimization of FeCrAl-based ODS alloy by machine learning combined with wedge-shaped hot-rolling. Materials Characterization, 2022, 188, 111894.	4.4	15
3	Revealing Microstructural, Textural, and Hardness Evolution of Ti–6Al–4V Sheet Cooled From Sub β-Transus Temperature at Different Rates. Metallurgical and Materials Transactions A: Physical Metallurgy and Materials Science, 2022, 53, 3179-3193.	2.2	10
4	Towards resolving a long existing phase stability controversy in the Zr-H, Ti-H systems. Journal of Nuclear Materials, 2021, 543, 152540.	2.7	10
5	Crystal Structure of Hydride Platelets in Hot Rolled Zircaloy-2, Characterized with Synchrotron X-Ray Diffraction, S/TEM, and EELS. , 2021, , 732-761.		2
6	Interstitialcy-based reordering kinetics of Ni3Al precipitates in irradiated Ni-based super alloys. Materialia, 2021, 19, 101180.	2.7	0
7	Stability of vacancy and interstitial dislocation loops in <mml:math xmlns:mml="http://www.w3.org/1998/Math/MathML" altimg="si24.svg"><mml:mi>α</mml:mi>-zirconium: atomistic calculations and continuum modelling, lournal of Nuclear Materials, 2021, 554, 153059.</mml:math 	2.7	11
8	Mechanisms for <100> interstitial dislocation loops to diffuse in BCC iron. Nature Communications, 2021, 12, 225.	12.8	22
9	Identifying the true structure and origin of the water-quench induced hydride phase in Zr-2.5Nb alloy. Acta Materialia, 2021, 221, 117369.	7.9	12
10	In situ TEM and multiscale study of dislocation loop formation in the vicinity of a grain boundary. Journal of Nuclear Materials, 2020, 528, 151872.	2.7	6
11	Influence of Al Addition Strategy on the Microstructure of a Lowâ€Cr Oxide Dispersionâ€Strengthened Ferritic Steel. Advanced Engineering Materials, 2020, 22, 1900879.	3.5	11
12	Oxidation behavior of 9Cr-4.5Al ODS steel in 600â€Â°C supercritical water and the effect of pre-oxidation. Corrosion Science, 2020, 165, 108380.	6.6	19
13	A method for calculation of bias factor in anisotropic mediums, application to αâ^'zirconium. Journal of Nuclear Materials, 2020, 528, 151882.	2.7	3
14	Accelerated kinetic Monte Carlo: A case study; vacancy and dumbbell interstitial diffusion traps in concentrated solid solution alloys. Journal of Chemical Physics, 2020, 153, 074109.	3.0	20
15	In-situ Observation of Irradiation Induced Defects in Fe and Fe-Cr Alloys. Microscopy and Microanalysis, 2020, 26, 886-886.	0.4	1
16	Tunable chemical complexity to control atomic diffusion in alloys. Npj Computational Materials, 2020, 6, .	8.7	37
17	Effect of He on the Order-Disorder Transition in Ni3Al under Irradiation. Physical Review Letters, 2020, 124, 075901.	7.8	9
18	Characterization of phases in the Zr–Nb–Fe ternary system at the Zr–Nb rich side of the phase diagram. Journal of Nuclear Materials, 2020, 534, 152142.	2.7	11

#	Article	IF	CITATIONS
19	Effects of pulsed laser surface treatments on microstructural characteristics and hardness of CrCoNi medium-entropy alloy. Philosophical Magazine, 2019, 99, 3015-3031.	1.6	14
20	A mechanism for basal vacancy loop formation in zirconium. Scripta Materialia, 2019, 172, 72-76.	5.2	19
21	Asymmetrical response of edge pyramidal dislocations in HCP zirconium under tension and compression: A molecular dynamics study. Computational Materials Science, 2019, 170, 109183.	3.0	8
22	Characterizing the crystal structure and formation induced plasticity of γ-hydride phase in zirconium. Materialia, 2019, 8, 100454.	2.7	14
23	Influences of Laser Surface Alloying with Cr on Microstructural Characteristics and Hardness of Pure Ti. Metallurgical and Materials Transactions A: Physical Metallurgy and Materials Science, 2019, 50, 3794-3804.	2.2	15
24	Mechanoelectrical Energy Conversion: Highly Efficient Mechanoelectrical Energy Conversion Based on the Nearâ€Tip Stress Field of an Antifracture Slit Observed in Scorpions (Adv. Funct. Mater. 22/2019). Advanced Functional Materials, 2019, 29, 1970147.	14.9	3
25	In-situ study of heavy ion irradiation induced lattice defects and phase instability in β-Zr of a Zr–Nb alloy. Journal of Nuclear Materials, 2019, 522, 192-199.	2.7	6
26	Microstructure Characterization and Mechanical Properties of Al Alloyed 9Cr ODS Steels with Different Al Contents. Steel Research International, 2019, 90, 1800594.	1.8	17
27	A direct comparison of annealing in TEM thin foils and bulk material: Application to Zr-2.5Nb-0.5Cu alloy. Materials Characterization, 2019, 151, 175-181.	4.4	11
28	Effect of the addition of Cu on irradiation induced defects and hardening in Zr-Nb alloys. Journal of Nuclear Materials, 2019, 519, 10-21.	2.7	9
29	Deformation-free nanotwin formation in zirconium and titanium. Materials Letters, 2019, 247, 111-114.	2.6	7
30	Highly Efficient Mechanoelectrical Energy Conversion Based on the Nearâ€Tip Stress Field of an Antifracture Slit Observed in Scorpions. Advanced Functional Materials, 2019, 29, 1807693.	14.9	21
31	Effect of Shear Strain Rate on Microstructure and Properties of Austenitic Steel Processed by Cyclic Forward/Reverse Torsion. Materials, 2019, 12, 506.	2.9	9
32	Effects of heavy ion irradiation on Zr-2.5Nb pressure tube alloy. II. Orientation dependent dislocation loop propagation and elemental redistribution. Journal of Applied Physics, 2019, 125, .	2.5	2
33	Irradiation damage and hardening in pure Zr and Zr-Nb alloys at 573†K from self-ion irradiation. Materials and Design, 2019, 161, 147-159.	7.0	33
34	Radiation effect on nano-indentation properties and deformation mechanisms of a Ni-based superalloy X-750. Journal of Nuclear Materials, 2019, 515, 1-13.	2.7	13
35	Combination of back stress strengthening and Orowan strengthening in bimodal structured Fe–9Cr–Al ODS steel with high Al addition. Materials Science & Engineering A: Structural Materials: Properties, Microstructure and Processing, 2019, 739, 45-52.	5.6	37
36	Primary damage production in the presence of extended defects and growth of vacancy-type dislocation loops in hcp zirconium. Physical Review Materials, 2019, 3, .	2.4	11

#	Article	IF	CITATIONS
37	Effect of pack-chromizing temperature on microstructure and performance of AISI 5140 steel with Cr-coatings. Surface and Coatings Technology, 2018, 344, 656-663.	4.8	24
38	Strengthening and toughening austenitic steel by introducing gradient martensite via cyclic forward/reverse torsion. Materials and Design, 2018, 143, 150-159.	7.0	36
39	<i>In situ</i> heavy ion irradiation in ferritic/martensitic ODS steels at 500°C. Materials Science and Technology, 2018, 34, 42-46.	1.6	6
40	Effect of pre-existing dislocations on the formation of dislocation loops: Pure magnesium under electron irradiation. Journal of Nuclear Materials, 2018, 511, 43-55.	2.7	19
41	A tomographic TEM study of tension-compression asymmetry response of pyramidal dislocations in a deformed Zr-2.5Nb alloy. Scripta Materialia, 2018, 153, 94-98.	5.2	17
42	Superfast Liquid Transfer Strategy Through Sliding on a Liquid Membrane Inspired from Scorpion Setae. Advanced Materials Interfaces, 2018, 5, 1800802.	3.7	11
43	Quantifying Irradiation Defects in Zirconium Alloys: A Comparison between Transmission Electron Microscopy and Whole-Pattern Diffraction Line-Profile Analysis. , 2018, , 691-724.		0
44	The habit plane of ã€^a〉-type dislocation loops in α-zirconium: an atomistic study. Philosophical Magazine, 2017, 97, 944-956.	1.6	15
45	Indentation behaviour of ion-irradiated X-750 Ni-based superalloy. Philosophical Magazine Letters, 2017, 97, 101-109.	1.2	10
46	The stability of thermodynamically metastable phases in a Zr-Sn-Nb-Mo alloy: Effects of alloying elements, morphology and applied stress/strain. Journal of Nuclear Materials, 2017, 493, 84-95.	2.7	7
47	Accumulation of dislocation loops in the $\hat{I}\pm$ phase of Zr Excel alloy under heavy ion irradiation. Journal of Nuclear Materials, 2017, 491, 232-241.	2.7	25
48	Effect of heavy ion irradiation on thermodynamically equilibrium Zr-Excel alloy. Journal of Nuclear Materials, 2017, 488, 33-45.	2.7	5
49	An embedded atom method interatomic potential for the zirconium-iron system. Computational Materials Science, 2017, 133, 6-13.	3.0	5
50	Spectral and raw quasi in-situ energy dispersive X-ray data captured via a TEM analysis of an ODS austenitic stainless steel sample under 1 MeV Kr 2+ high temperature irradiation. Data in Brief, 2017, 14, 707-712.	1.0	2
51	Stacking faults observed in {10 <mml:math <br="" xmlns:mml="http://www.w3.org/1998/Math/MathML">altimg="si1.gif" overflow="scroll"><mml:mover accent="true"><mml:mn>1</mml:mn><mml:mo stretchy="true">â^`</mml:mo </mml:mover></mml:math> 2} extension twins in a compressed high Sn content Zr alloy. Scripta Materialia, 2017, 141, 72-75.	5.2	13
52	Quasi in-situ energy dispersive X-ray spectroscopy observation of matrix and solute interactions on Y Ti O oxide particles in an austenitic stainless steel under 1ÂMeV Kr2+ high temperature irradiation. Acta Materialia, 2017, 141, 241-250.	7.9	6
53	Atomistic simulations of Ni segregation to irradiation induced dislocation loops in Zr-Ni alloys. Acta Materialia, 2017, 140, 56-66.	7.9	22
54	A test of a phenomenological model of size dependent melting in Au nanoparticles. Acta Materialia, 2017, 136, 11-20.	7.9	22

ZHONGWEN YAO

#	Article	IF	CITATIONS
55	Precipitate Stability in a Zr–2.5Nb–0.5Cu Alloy under Heavy Ion Irradiation. Metals, 2017, 7, 287.	2.3	13
56	Irradiation Induced Defect Clustering in Zircaloy-2. Applied Sciences (Switzerland), 2017, 7, 854.	2.5	6
57	<i>In situ</i> transmission electron microscopy study of the thermally induced formation of δ′-ZrO in pure Zr and Zr-based alloy. Journal of Applied Crystallography, 2017, 50, 1028-1035.	4.5	13
58	Zirconium hydrides and Fe redistribution in Zr-2.5%Nb alloy under ion irradiation. Journal of Nuclear Materials, 2016, 480, 332-343.	2.7	19
59	Study of microstructure and precipitates of a Zr-2.5Nb-0.5Cu CANDUÂspacer material. Journal of Nuclear Materials, 2016, 481, 153-163.	2.7	20
60	Direct determination of trace elements in austenitic stainless steel samples by ETV-ICPOES. Journal of Analytical Atomic Spectrometry, 2016, 31, 2434-2440.	3.0	17
61	Atomistic simulations of the formation of <c>-component dislocation loops in α-zirconium. Journal of Nuclear Materials, 2016, 478, 125-134.</c>	2.7	30
62	Metastable phases in Zr-Excel alloy and their stability under heavy ion (Kr2+) irradiation. Journal of Nuclear Materials, 2016, 469, 9-19.	2.7	13
63	Effects of alloying elements on the formation of < <i>c</i> >-component loops in Zr alloy Excel under heavy ion irradiation. Journal of Materials Research, 2015, 30, 1310-1334.	2.6	19
64	Deformation mechanism study of a hot rolled Zr-2.5Nb alloy by transmission electron microscopy. II. <i>In situ</i> transmission electron microscopy study of deformation mechanism change of a Zr-2.5Nb alloy upon heavy ion irradiation. Journal of Applied Physics, 2015, 117, .	2.5	9
65	Deformation mechanism study of a hot rolled Zr-2.5Nb alloy by transmission electron microscopy. I. Dislocation microstructures in as-received state and at different plastic strains. Journal of Applied Physics, 2015, 117, 094307.	2.5	13
66	Dislocation-accelerated void formation under irradiation in zirconium. Acta Materialia, 2015, 82, 94-99.	7.9	26
67	Cavity morphology in a Ni based superalloy under heavy ion irradiation with hot pre-injected helium. II. Journal of Applied Physics, 2014, 115, 103509.	2.5	11
68	Cavity morphology in a Ni based superalloy under heavy ion irradiation with cold pre-injected helium. I. Journal of Applied Physics, 2014, 115, 103508.	2.5	13
69	Microstructure evolution during electron and ion irradiation in commercial purity magnesium. Philosophical Magazine, 2014, 94, 1909-1923.	1.6	5
70	Spatial ordering of nano-dislocation loops in ion-irradiated materials. Journal of Nuclear Materials, 2014, 455, 16-20.	2.7	58
71	Radiation induced microstructures in ODS 316 austenitic steel under dual-beam ions. Journal of Nuclear Materials, 2014, 455, 242-247.	2.7	16
72	Stability of Ni3(Al, Ti) Gamma Prime Precipitates in a Nickel-Based Superalloy Inconel X-750 Under Heavy Ion Irradiation. Metallurgical and Materials Transactions A: Physical Metallurgy and Materials Science, 2014, 45, 3422-3428.	2.2	21

#	Article	IF	CITATIONS
73	TEM characterization of in-reactor neutron irradiated CANDU spacer material Inconel X-750. Journal of Nuclear Materials, 2014, 451, 88-96.	2.7	44
74	Convoluted dislocation loops induced by helium irradiation in reduced-activation martensitic steel and their impact on mechanical properties. Materials Science & Engineering A: Structural Materials: Properties, Microstructure and Processing, 2014, 607, 390-396.	5.6	21
75	Elevated temperature irradiation damage in CANDU spacer material Inconel X-750. Journal of Nuclear Materials, 2014, 445, 227-234.	2.7	24
76	Novel techniques of preparing TEM samples for characterization of irradiation damage. Journal of Microscopy, 2013, 252, 251-257.	1.8	3
77	Microstructural evolution of CANDU spacer material Inconel X-750 under in situ ion irradiation. Journal of Nuclear Materials, 2013, 443, 49-58.	2.7	51
78	In situ study of defect accumulation in zirconium under heavy ion irradiation. Journal of Nuclear Materials, 2013, 433, 95-107.	2.7	65
79	Molecular dynamics simulations of irradiation cascades in alpha-zirconium under macroscopic strain. Nuclear Instruments & Methods in Physics Research B, 2013, 303, 95-99.	1.4	38
80	Ion irradiation-induced precipitation of Cr23C6 at dislocation loops in austenitic steel. Scripta Materialia, 2013, 68, 138-141.	5.2	32
81	Irradiation induced microstructural changes in Zr-Excel alloy. Journal of Nuclear Materials, 2013, 441, 138-151.	2.7	29
82	Effect of foil orientation on damage accumulation during irradiation in magnesium and annealing response of dislocation loops. Journal of Nuclear Materials, 2012, 423, 132-141.	2.7	16
83	In situ transmission electron microscopy and ion irradiation of ferritic materials. Microscopy Research and Technique, 2009, 72, 182-186.	2.2	52
84	Dynamic observations of heavy-ion damage in Fe and Fe–Cr alloys. Journal of Nuclear Materials, 2009, 389, 197-202.	2.7	146
85	Shape of prismatic dislocation loops in anisotropic <i>α</i> -Fe. Philosophical Magazine Letters, 2009, 89, 581-588.	1.2	28
86	Preparation of TEM samples of ferritic alloys. Journal of Electron Microscopy, 2008, 57, 91-94.	0.9	16
87	Synergistic effects of PKA and helium on primary damage formation in Fe–0.1%He. Journal of Nuclear Materials, 2007, 367-370, 462-467.	2.7	15
88	Irradiation induced behavior of pure Ni single crystal irradiated with high energy protons. Journal of Nuclear Materials, 2003, 323, 388-393.	2.7	26
89	The behavior of coatings and SiCf/SiC composites under thermal shock. Journal of Nuclear Materials, 2000, 283-287, 1077-1080.	2.7	8